# Influence of the atmospheric stratification on the sound propagation of single flights

Christoph ZELLMANN[1]; Jean Marc WUNDERLI[2]

[1-2] Empa, Switzerland

## ABSTRACT

Aircraft noise models generally simplify the atmosphere as homogenous and constant over time. However, momentary local conditions of wind, humidity and temperature influence the sound exposure level and become relevant for the calculation of single flights.

This paper presents a method to classify the atmospheric conditions with idealized vertical profiles derived from weather data of a monitoring station in combination with a radiation balance. The differences of the propagation in a homogenous and a stratified atmosphere are analyzed by exemplary overflights. Additionally, the attenuations due to idealized profiles are compared to those of vertical profiles obtained from flight data records and profiles from a meteorological prediction model.

The comparison between the different profiles shows good agreement for temperature, except for the transition between stable and unstable stratification, but larger deviations for humidity. Furthermore it can be shown that the reproduction of a stratified atmosphere in the propagation calculation has a beneficial effect on the accuracy of the resulting sound exposure level and should therefore be taken into account for sophisticated aircraft noise modelling. Therefore, input data of a meteorological prediction model should be used where available, as idealized profiles do not always reproduce the atmosphere accurately.

Keywords: Sound propagation, Aircraft noise, Modelling
I-INCE Classification of Subjects Numbers: 24.6, 76.1.3

## 1. INTRODUCTION

Sound propagation through the atmosphere is influenced by local conditions of temperature, humidity and wind speed. For aircraft noise the predominant meteorological effect on sound propagation is dissipation. Second order effects include level fluctuations caused by turbulence and on rare occasions with sound paths close to the ground the evolution of acoustical shadow zones and influences on barrier effects as a consequence of temperature and wind gradients with height.

Many aircraft noise models (1, 2) have been developed with the purpose of calculating yearly air traffic scenarios. In general the motives are either to reproduce current situations for legal compliance purposes or to study future situations as a basis for land-use planning. Here, the atmosphere is usually represented in a highly simplified way as being homogenous and constant over time. Such a simplification seems to be valid for yearly scenarios. Binder showed that the effect of changing atmospheric conditions on A-weighted level tends to average out over time (3).

Other aircraft noise models (4, 5) are developed with the aim of detailed noise calculations for single flights and the optimization of flight procedures. For such applications the source models have to be more detailed, but also the propagation models have to be more sophisticated, including a momentary representation of the atmosphere.

Another aircraft noise model for single flights, called *sonAIR*, is currently developed at the authors' institution (6). A key element is the separation of the source model and the propagation model. The source model is based on a semi-empirical approach and will account for airframe and engine noise of different flight conditions. The sound propagation model, called *sonX*, has been developed in previous projects and has so far been applied for railway noise (7, 8) and shooting noise (9). *sonX* is currently adapted to the specific issues of aircraft noise calculations. Apart from the detailed propagation

---

calculation for the prognosis of single flights it is also used to reversely transform measured data at the receiver to the source. Here, the exact atmospheric reproduction is particularly crucial.

A sophisticated propagation model also requires a higher level of detail and quality of the input data. Appropriate data of the vertical profile of the atmosphere can be obtained from different sources:

- From weather balloons or from measurements of the aircraft itself.
- From simulation results of numerical weather prediction models such as COSMO for many European countries (10).
- Based on measurements of ground stations, in combination with idealized profiles.

In this paper we present and compare meteorological data from the three different sources and assess their impact on the resulting sound attenuation for different source-receiver-geometries. In section 2 a method is described to derive idealized profiles from meteorological data of ground stations. Based on these results the benefit of a detailed modelling of the atmosphere is discussed in comparison with the assumption of a homogenous atmosphere.

## 2. METHODS

### 2.1 Propagation model

All propagation calculations in the present paper were done by the *sonX* model. The calculation from a point source to a receiver is conducted in two steps. First, the direct sound propagation for a uniform atmosphere with averaged conditions is calculated according to Eq. (1). It accounts for geometrical divergence ($A_{div}$) and atmospheric dissipation ($A_{atm,f}$) in dependence of the frequency $f$ according to ISO 9613-1 (11). The model also accounts for barrier and ground effects ($A_{gr/bar,f}$) as well as foliage attenuation ($A_{fol,f}$), which are negligible for the consideration in this paper.

$$A_{Basic,f} = A_{div} + A_{atm,f} + A_{gr/bar,f} + A_{fol,f} \qquad (1)$$

Second, additional meteorological effects like atmospheric dissipation ($A_{atm,Meteo}$) due to local temperature and humidity conditions are calculated by Eq. (2). The attenuations are reported in level differences in comparison to the basic attenuations of Eq. (1). In addition, changes of shielding effects and the evolution of acoustical shadow zones due to temperature and wind gradients ($D_{met}$) are calculated by using a ray tracing algorithm. These effects are not relevant for the current analysis.

$$A_{Meteo} = (A_{atm,Meteo} - A_{atm,Basic}) + (A_{fol,Meteo} - A_{fol,Basic}) - D_{met} \qquad (2)$$

The *sonX* model also includes models for reflections at buildings, walls and other rigid surfaces as well as diffuse reflections at forest edges and cliffs. However these parts are also not relevant in this context and are therefore omitted here. For a detailed description as well as further references of the propagation model we refer to (9, 12).

Information about the vertical profile of the atmosphere can be supplied as individual profiles (i.e. from prediction models or flight record data) or as idealized profiles (cf. Sec. 2.3). For the latter a classification scheme has been introduced (Table 1). The classification is based on the scheme of Polster (13), but reduced to the three main classes unstable (U), neutral (N) and stable (S). Depending on the wind speed at 10 m height and the current radiation balance a corresponding class can be determined for any specific atmospheric condition.

Table 1 – Classification scheme for different weather conditions

| Wind speed $v$, m/s | | Radiation balance $Q$ | | |
|---|---|---|---|---|
| Range | **Average** | Unstable | Neutral | Stable |
| | | $< -18$ W/m$^2$ | | $> 180$ W/m$^2$ |
| 0-1 | **0.0** | U0 | N0 | S0 |
| 1-2 | **1.5** | U1 | N1 | S1 |
| 2-3 | **2.5** | U2 | N2 | S2 |
| 3-5 | **4.0** | U3 | N3 | S3 |
| >5 | **6.0** | U4 | N4 | S4 |

## 2.2    Radiation balance and development of idealized profiles

The measurement of the radiation balance is possible but not always available as several sensors are needed. In Switzerland typically only the incoming short-wave radiation is available, measured by a Pyranometer. Therefore, the determination of the radiation balance follows the VDI-Standard 3789 Part 2 (14). Regarding a horizontal area the radiation balance is the sum of the solar short-wave and terrestrial long-wave radiation, Eq. (3). The solar short-wave radiation is the difference of the global radiation ($G$) and its reflection ($R$) which depends on the short-wave albedo of the earth's surface. The emitted thermal radiation ($E$) of the earth can be simplified for natural ground surfaces as a black body that emits energy with the fourth power to the surface temperature. Atmospheric gases and clouds reflect back to the earth ($A$).

$$Q = (G - R) + (A - E) \tag{3}$$

The radiation balance was calculated for each day of the acoustical measurements (15) to collect *sonAIR* source data (Figure 1, top). Weather data at station height (Station KLO at airport Zurich, 426 m above MSL) in ten minutes resolution was used as input for the radiation balance. The cloud cover $N$ in eights is a visually observed parameter with a resolution of one hour, thus it was interpolated by a piecewise cubic hermite interpolating polynomial to guarantee a smooth curve of the counterradiation. By means of the radiation balance and the wind speed the classification scheme from Table 1 was implemented as shown in Figure 1 (bottom).

For each class in Table 1, predefined LinLog-profiles of the temperature, wind and humidity have been calculated (16), which represent idealized profiles for the meteorological class and different ground types. For the application under specific conditions the profiles were shifted towards the current temperature and humidity at the ground. The weather data used here had reference heights of 2 meters for temperature and humidity and 6 meters for wind direction. The profiles show considerable variations close to the ground. However, towards greater heights (more than 100 m) they exhibit a uniform behaviour with constant wind speed and direction, and an adiabatic lapse rate of 9.8 K/km for unsaturated air respectively 6.5 K/km for saturated air. Absolut humidity is assumed to be unchanged and hence relative humidity increases with height up to a maximum of 100%.
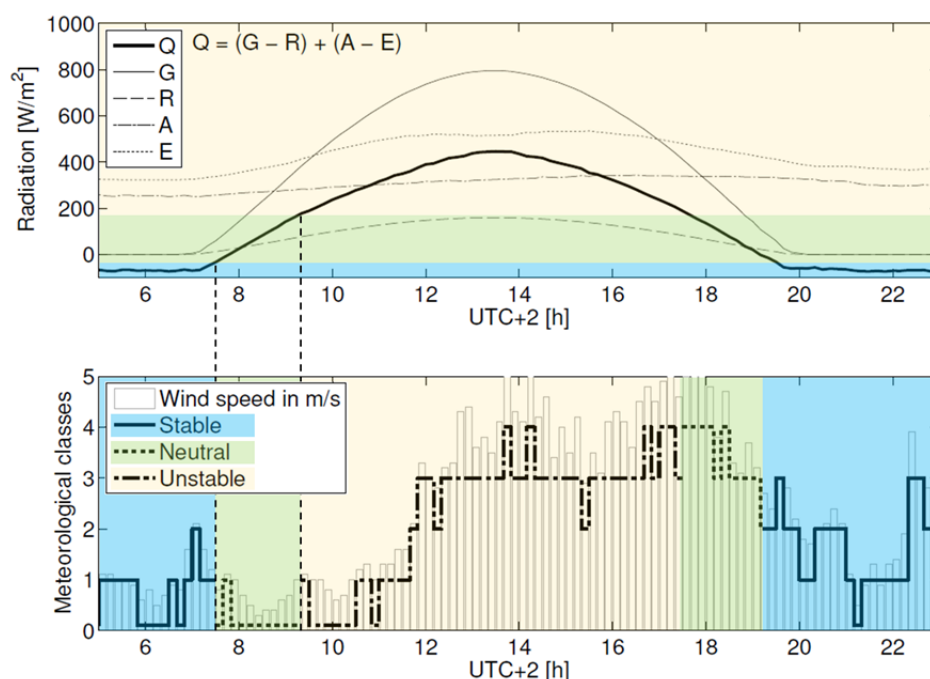


Figure 1 – Radiation balance for an exemplary day in September 2013 at Zurich airport (top). In combination with the wind speed the meteorological classes represent the different conditions during daytime (bottom).

## 2.3    Profile data

The study includes flight data records (FDR) for 223 departures at Zurich airport, which are provided by Swiss International Airlines for the *sonAIR* project. From this data, the air temperature and the wind speed and its direction were processed to create vertical profiles like in Figure 2. In *sonAIR* the FDR will further be processed in combination with the acoustical measurements (15) to develop the sound emission model in function of the flight configuration.

All data considered in this paper originate from flights that have been measured within four weeks between August 21 and September 13 in 2013. Most of the departures of the A320-family took place at daytime between 9 a.m. and 4 p.m. While variations of atmospheric conditions are therefore limited, the temperatures still varied between 12°C and 28°C and the humidity between 20% and 80%. In addition ten flights of the A340-300 and three other types were measured at night around 11 p.m., where the temperature was still around 17°C to 20°C and the humidity some 65%.

As an alternative, profile data of the numerical weather prediction model COSMO-2 was used as input data for the propagation calculation. COSMO is the Consortium for Small-Scale Modelling of the national weather services of Germany, Greece, Italy, Poland, Romania, Russia, and Switzerland (10). MeteoSwiss, who provided the data, uses the local scale model COSMO-2 with a grid spacing of 2.2 km, which also includes the Alpine arc (17). In fact, the numerical model assimilates atmospheric observation data from radiosonde, aircraft, wind profiler, and surface-level data. The provided hourly profiles include temperature, humidity, and wind speed and direction for the level-surfaces 24 to 60 equaling heights above ground of approx. 10 m to 4900 m.

In Figure 2 the four types of profiles are exemplarily compared with each other. For a comparison with a homogenous atmosphere based on momentary conditions, weather data at Zurich airport was used at a reference height of 2 m and is also plotted over height. Figure 2 shows an unstable situation at 10 a.m., for which all data sources show a similar pattern over the entire range of height up to 800 m. In contrast Figure 3 depicts a situation where the different profiles deviate considerably. The temperature decreases with increasing height for the COSMO-2 and FDR profiles, indicating an unstable stratification. In contrast the idealized profile already assumes a neutral condition. In the same way the humidity profiles differ strongly.
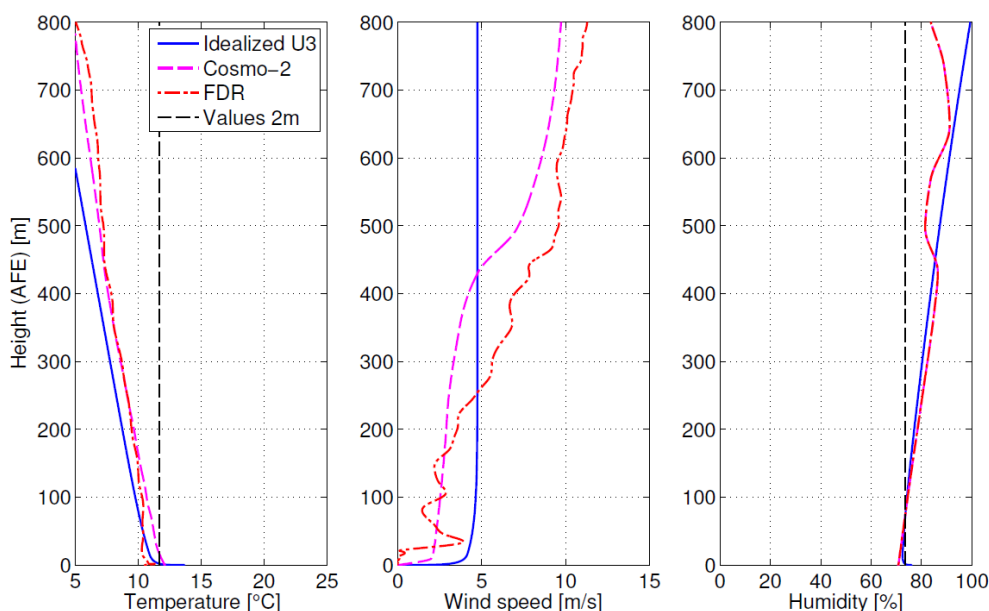


Figure 2 – Temperature, wind and humidity profiles for an exemplary day at 10 a.m. in September 2013 at Zurich airport. This example shows idealized profiles (blue solid line) in good agreement with profiles from the numerical model COSMO-2 (magenta dashed line) and FDR data (red dash-dotted line). The dashed black line represents a homogenous atmosphere with values measured at station height.
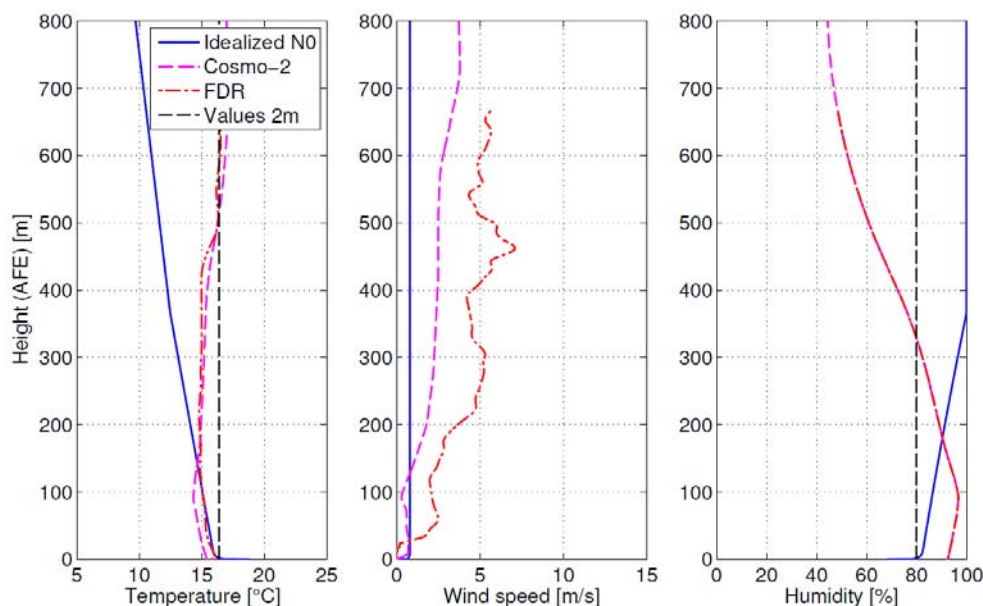
Figure 3 – Temperature, wind and humidity profiles for an exemplary day at 9 a.m. in September 2013 at Zurich airport. This example shows idealized profiles (blue solid line) in high divergence to profiles from the numerical model COSMO-2 (magenta dashed line) and FDR data (red dash-dotted line). The dashed black line represents a homogenous atmosphere with values measured at station height.

Further, the idealized profiles could not always reproduce the temporal transition of a stable boundary layer at night to a typically unstable layer at a sunny day correctly. In Figure 4 the vertical profiles of the idealized profiles and COSMO-2 data are compared for three different times of the day between 9.30 a.m. and noon. For this sunny day (see Figure 1) the sun rises already at 7.30 a.m. and the radiation balance leads to an unstable stratification already 2 hours later if the classification scheme is applied. In contrast, the data of COSMO-2 indicate that the change of the stratification up to 500 m is still ongoing until noon, the temperature and humidity profiles converge only slowly.
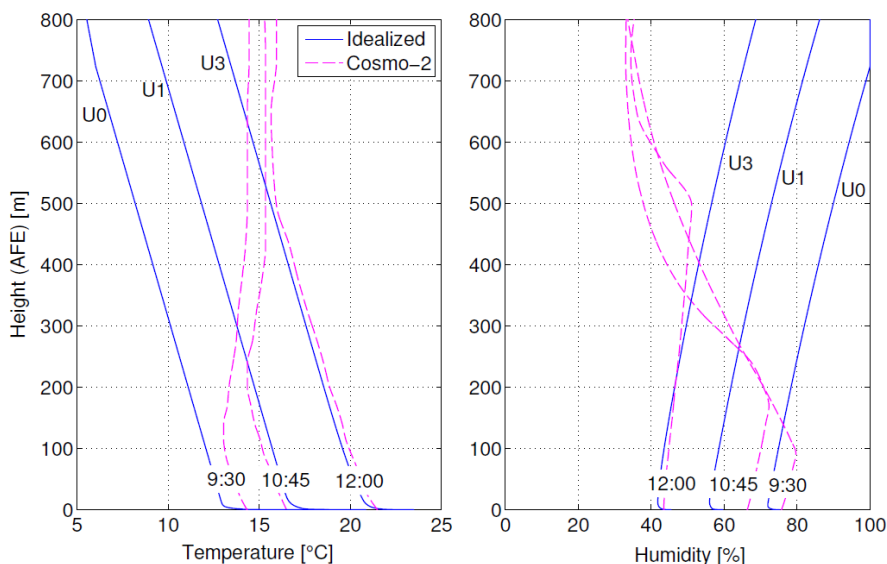


Figure 4 – Selected temperature and humidity profiles for an exemplary day between 9 a.m. and 12 noon in September 2013 at Zurich airport. The numerical model COSMO-2 (magenta dashed line) indicates that the stratification from a stable boundary layer at night to a typically unstable layer at a sunny day is still ongoing until noon. The classification scheme already assumes an unstable stratification (blue solid line).

In summary, FDR and COSMO-2 profiles of wind and temperature are generally highly consistent. The extrapolation of temperature from ground conditions to greater heights as performed by the idealized profiles seems to be valid in most cases. However wind and humidity profiles differ significantly compared to the more sophisticated profiles from the COSMO-2 model.

## 2.4    Propagation calculation

In this paper only the influence of the atmosphere on sound propagation shall be analyzed. Although the flight path of the 223 used departures is available, the same generic source points from a virtual flight path have been used for all flights to avoid differences in propagation due to different flight path geometry. The scenario depicted in Figure 5 shows the three different source positions (S), one 500 m above receiver $R_1$ and the others in 45° and 30° angle with respect to the flight direction. A second receiver $R_2$ was set 500 m sidewise. The receivers are set 4 m above a plain grassland terrain.
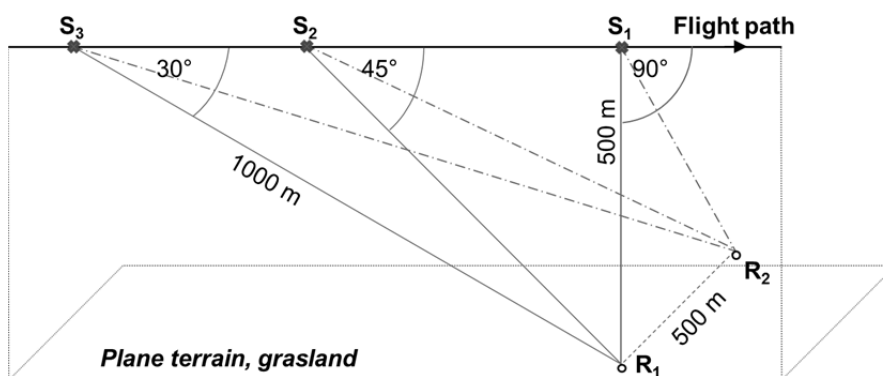


Figure 5 – Calculation scenario

In the following, the results are presented as attenuations $A_{Meteo}$ (Eq. (2)) of the propagation calculation to show the differences between a homogenous atmosphere based on momentary local conditions (LC) and on averaged conditions for Switzerland. Furthermore the results of the COSMO-2 data are compared to those of the homogenous atmosphere based on momentary conditions (Eq. (4)). In addition the results of the idealized standard profiles (IP) are compared to those of COMSO-2 profiles (Eq.(5)). The differences of the attenuations for each one-third octave band up to 5 kHz are shown in Sec. 3.1 and 3.2. In Sec. 3.3 the influence on the A-weighted sound exposure level $L_{AE}$ is discussed.

As FDR data do not provide information on humidity data, this information was taken from COMSO-2 for the sound propagation calculation. However the results turned out to be very similar to the calculations with COSMO-2 profiles and are therefore not shown and discussed further.

$$\Delta A_{LC-COSMO} = A_{Meteo,LC} - A_{Meteo,COSMO} \tag{4}$$

$$\Delta A_{IP-COSMO} = A_{Meteo,IP} - A_{Meteo,COSMO} \tag{5}$$

# 3.   RESULTS

Distributions of the calculated differences of air absorption are presented for the 223 departures respectively their assigned meteorological situations. For each one-third octave band the differences are shown as Box-Whiskers-plots (cf. legend in Figure 6). Providing the most reliable data COMSO-2 will be used as reference for the comparison of results.

## 3.1    Differences between homogenous atmospheres

In a first step, the attenuation of a homogenous atmosphere based on momentary conditions at the ground is compared to the attenuation of homogenous atmosphere with averaged values of 8°C and 76% for Switzerland. The results for the closest point of approach (CPA) in Figure 6 showed only minor variations less than 0.6 dB below 500 Hz. Between 500 Hz and 1.6 kHz mean values of approx. +0.5 dB resulted with maximum values of +1.9 dB and positive minima (except for 1.6 kHz). Hence the momentary conditions always led to higher attenuations than the averaged atmosphere. For high

frequencies the trend changed to negative differences but showed much higher variations in both directions. The mean value of the 5-kHz-band was –4.3 dB with a minimum value of –10.3 dB and a maximum of +15.0 dB.

Figure 7 shows the attenuation spectra for the largest propagation distance of 1118 m. The same trend is observed as for the CPA with a turn to negative values at 2 kHz. The mean values for 500 Hz to 1.6 kHz ranged from +0.5 dB to +1.0 dB with maximal values from +2.0 dB to +4.3 dB and also positive minima. The high frequencies showed higher negative mean dissipation for an atmosphere based on momentary conditions, again with large deviations between –23 dB to +34 dB.
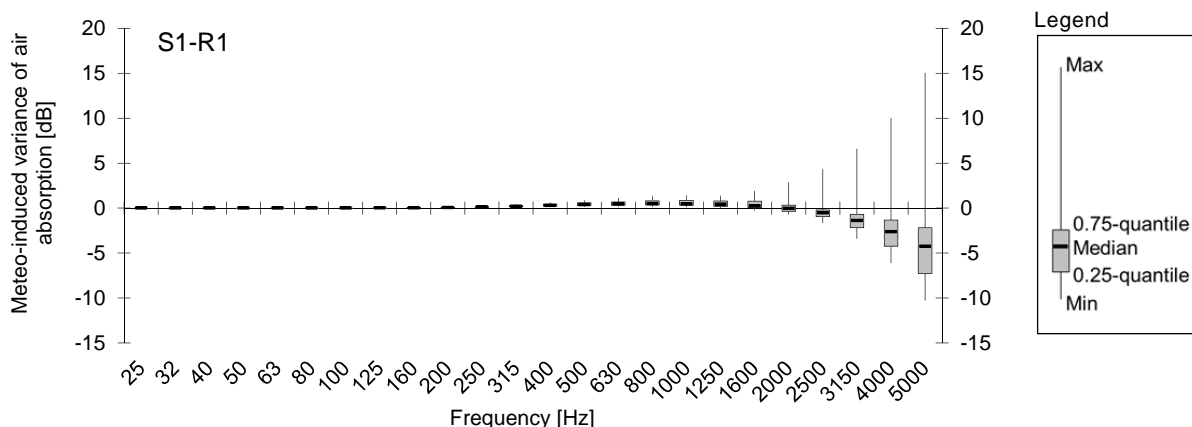


Figure 6 – Variation of air absorption of a homogenous atmosphere shifted to momentary conditions at 2 m to a uniform atmosphere with averaged conditions. Results for the propagation S1 to R1 at 500 m distance.
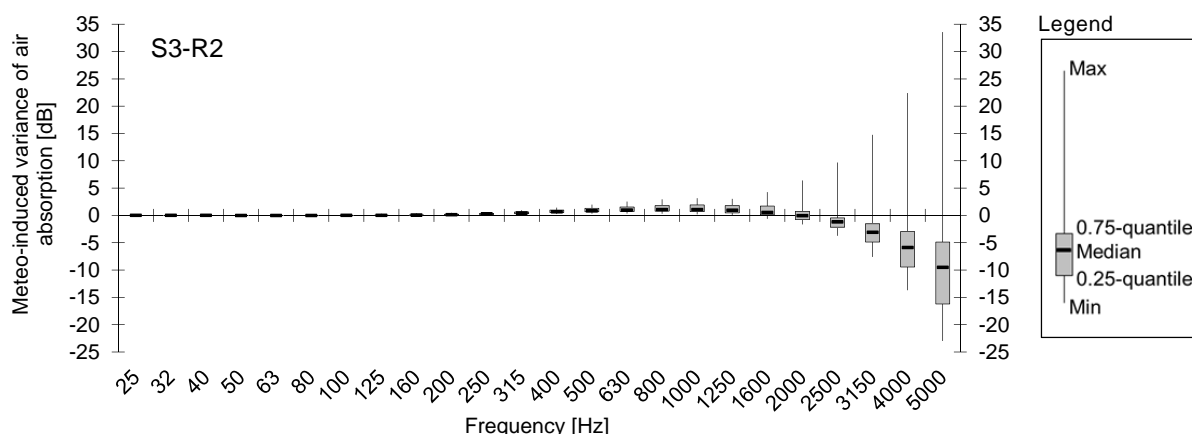


Figure 7 – Variation of air absorption of a homogenous atmosphere shifted to momentary conditions at 2 m to a uniform atmosphere with averaged conditions. Results for the propagation S3 to R2 at 1118 m distance.

## 3.2 Differences of the profile data sources

In this section the results are presented only for 250 Hz to 5 kHz because the variation of low frequencies is negligible. Figure 8 (left) shows the variations in air absorption between the homogenous atmosphere at momentary conditions and the COSMO-2 profiles for S1 to R1. Below 2 kHz the mean values were slightly positive. In contrast, above 2 kHz the mean differences increased up to –3.6 dB for 5 kHz with large variations of –17.4 dB to +5.7 dB. Figure 8 (right) compares the propagation from S3 to R2. The trend is similar, but with larger variations for mid and high frequencies as a consequence of the greater propagation distance.

The variance of the idealized profiles compared to the COMSO-2 profiles is presented in Figure 9. For both spectra there were no variations higher than 0.5 dB below 1 kHz. For higher frequencies the mean values for Figure 9 (left) decreased to 4.2 dB at 5 kHz varying from –17.3 dB to 2.3 dB. In Figure 9 (right) the mean values also decreased to 3.4 dB but varied from –15.1 dB to 8.1 dB.
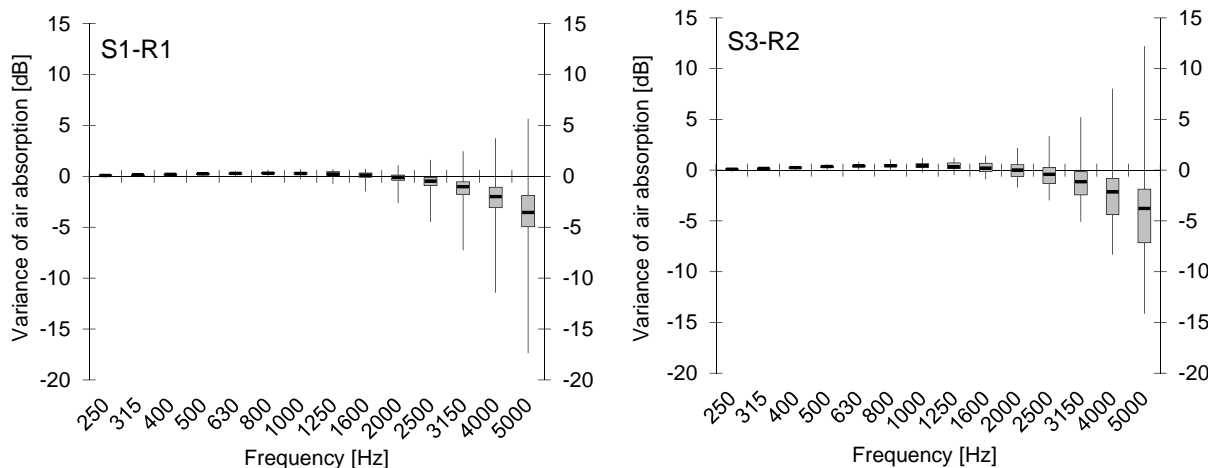
Figure 8 – Differences in air absorption between a homogenous atmosphere at momentary conditions and COSMO-2 profiles. Results for the propagation S1 to R1 (500 m) and S3 to R2 (1118 m).
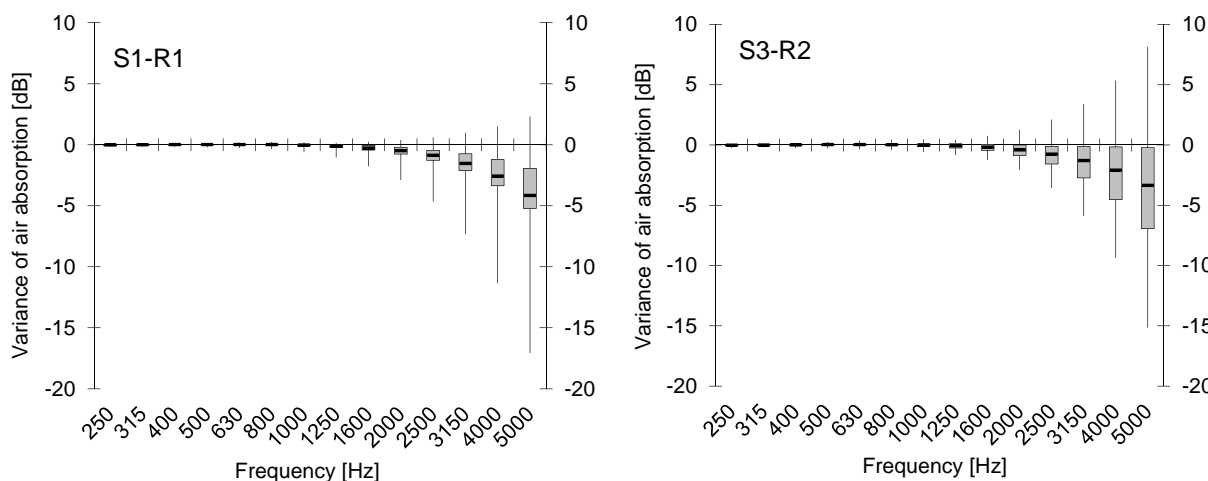


Figure 9 – Differences in air absorption between idealized profiles and COSMO-2 profiles. Results for the propagation S1 to R1 (500 m) and S3 to R2 (1118 m).

### 3.3  Influence on the resulting sound exposure level

The results in Sec. 3.1 demonstrate considerable variations of air absorption for frequencies above 250 Hz. The question thus arises how relevant these variations are for the resulting $L_{AE}$. Therefore sound emission directivities of 35 Airbus A320 were averaged and the resulting A-weighted spectra as well as the total $L_{AE}$ at receiver R1 were calculated (Figure 10). Then, the differences to the $L_{AE}$ were determined for the mean difference and minimal and maximal variations of Sec. 3.1.

Variations at frequencies above 2.5 kHz have almost no influence on the $L_{AE}$ (<0.1 dB(A)), particularly due to the high absolute atmospheric absorption. The same applies for frequencies below 125 Hz that are highly attenuated by the A-weighting. The influence between a homogenous atmosphere at local and average conditions on the $L_{AE}$ for 500 m (S1R1) is –0.2 dB(A) as a mean but varies from –1.4 dB(A) to 0.3 dB(A) for single flights. At 1000 m (S3R1) the mean variation on the $L_{AE}$ is –0.6 dB(A) with a range from –2.6 dB(A) to 0.2 dB(A).

In the same way the influence of the differences in air absorption between a homogenous atmosphere at momentary conditions and COSMO-2 profiles are –0.6 dB(A) to 1.3 dB(A) at 500 m and –0.9 dB(A) to 0.4 dB(A) at 1000 m. The differences in calculated air absorption of idealized and COSMO-2 profiles change the $L_{AE}$ from –0.2 dB(A) to 1.5 dB(A) at 500 m and from –0.5 dB(A) to 0.7 dB(A) at 1000 m.

As Figure 9 shows, the differences between idealized and COSMO-2 profiles at frequencies above 1 kHz are of the same order of magnitude as the variance between the homogenous atmosphere at momentary conditions and COMSO-2. However, for mid-frequencies below 1 kHz, which strongly influence the $L_{AE}$, the variations are small.
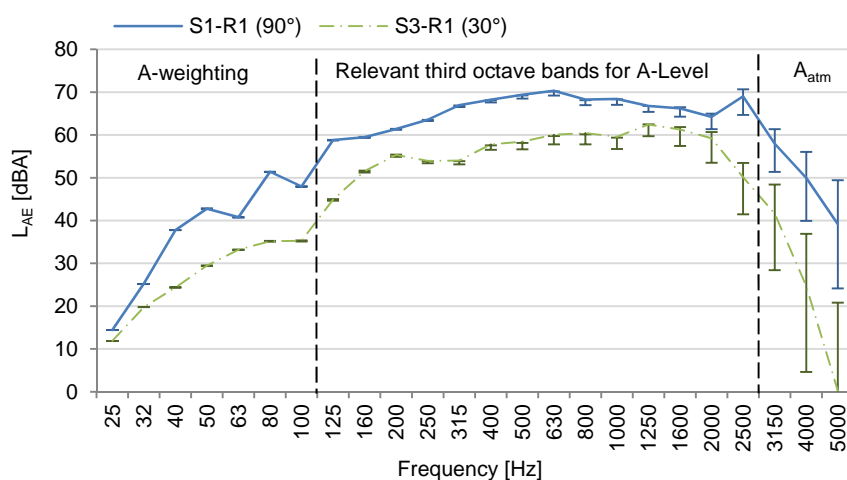
Figure 10 – Influence of the variance of dissipation on the A-weighted spectrum at the receiver R1 of the A320 for the incidence from S1 (90°) and from the front at S3 (30°). The indicators represent the minimal and maximal variations between the homogenous atmospheres at momentary resp. averaged conditions.

## 4.  DISCUSSION

In this study, a considerable dependence of the sound level at higher frequencies on varying conditions of temperature and humidity were found. For the frequency bands considerably effecting the resulting A-weighted level the differences are smaller but still in the range of several decibel. Looking at the mean values it can be seen that the deviations between the different datasets show a clear trend, hence having a systematic influence also on the resulting long-term averages.

Comparing the different sources for meteorological data, prediction models such as COSMO-2 seem most reliable. While FDR data are in good agreement with COSMO-2 for wind and temperature (Sec. 2.3), they provide no humidity data. In addition to the fact that FDR-data cannot be used as sole data source, the availability of FDR data is usually restricted and also the accuracy of input data depends on the type of aircraft. Therefore FDR data alone is not an appropriate source for meteorological data.

The use of standardized profiles of the atmosphere which are normalized to conditions at the ground as shown in Sec. 2.2 has a beneficial effect on the accuracy of the sound propagation calculation compared to the assumption of a homogenous atmosphere. The advantage of this approach is that profiles can be generated with very few, easily accessible input data. However the identified weakness in reproducing correct humidity profiles leads to considerable differences of the resulting air absorptions compared to calculations based on COSMO-2 data.

When generalizing the results, one must consider that this study its base on data of four weeks in late summer only. For cold and dry days the trend of the differences between homogenous atmospheres may reverse. However, the variance of air absorption is expected to be of the same order of magnitude as the results presented here. In contrast, the variations between the homogenous atmosphere at momentary conditions and idealized profiles to the COSMO-2 profiles are not expected to change considerably and the following conclusions can also be regarded as generally applicable.

## 5.  CONCLUSIONS

The use of momentary ground conditions of temperature and humidity is an important improvement compared to a uniform atmosphere with averaged conditions for the calculation of single flights. Additionally a correct reproduction of the stratification in the propagation calculation has again a beneficial effect on the accuracy of the resulting $L_{AE}$. In particular, the use of data from weather prediction models such as COSMO-2 is assumed to be the most accurate solution. Specifically for the development of the emission model, in which single flight events are reversely transformed to the source, it is recommended to make use of such detailed input data. Although high frequencies over 2.5 kHz are negligible for the $L_{AE}$ above 500 m, the large variation of the air absorption could lead to large errors in this band.

It turned out that idealized profiles are not able to replace the more detailed profiles from COSMO-2. The assumptions, particularly for the humidity but also for the temperature above 100 m often lead to an extrapolation of the ground conditions, which is not valid for greater heights. Hence, the differences in air absorption compared to the COSMO-2 profiles, which are considerable for frequencies above 1 kHz, change the $L_{AE}$ and result in a less accurate prognosis for single flights.

## ACKNOWLEDGEMENTS

## REFERENCES

1. Boeker ER, Dinges E, He B, Fleming G, Roof CJ, Gerbi PJ, et al. Integrated Noise Model (INM), Version 7.0, Technical Manual. Report No. FAA-AEE-08-01. Washington, DC: Federal Aviation Administration (FAA), U.S. Department of Transportation; 2008.
2. Pietrzko S, Hofmann RF. Prediction of A-weighted aircraft noise based on measured directivity patterns. Applied Acoustics. 1988;23(1):29-44. PubMed PMID: ISI:A1988L824400003.
3. Binder U, Isermann U, Schmid R. Influence of real atmospheric conditions on free propagation of aircraft noise. Acta Acustica united with Acustica. 2013;99(2):192-200.
4. Lopes LV, Burley CL, editors. Design of the next generation aircraft noise prediction program: ANOPP22011; Portland, OR.
5. Huemer RG, König R, Friehmelt H, Isermann U, Boguhn O, editors. The influence of modern noise-simulation-tools on the design of future noise-abatement-approach-procedures. Collection of Technical Papers - AIAA Guidance, Navigation, and Control Conference; 2004.
6. Schäffer B, Zellmann C, Krebs W, Plüss S, Eggenschwiler K, Bütikofer R, et al., editors. Sound source data for aircraft noise calculations – state of the art and future challenges. Proceedings of Euronoise 2012, Ninth European Conference on Noise Control; 2012 June 10-13, 2012; Prague, Czech Republic.
7. Sehu D, Wunderli JM, Heutschi K, Thron T, Hecht M, Rohrbeck A, et al. sonRAIL - Projektdokumentation: BAFU, Empa; 2010 [updated 7.10.2010]. Available from: http://www.empa.ch/plugin/template/empa/*/102455.
8. Thron T, Hecht M. The sonRAIL emission model for railway noise in Switzerland. Acta Acustica United with Acustica. 2010;96:873 - 83.
9. Wunderli JM, Pieren R, Heutschi K. The Swiss shooting sound calculation model sonARMS. Noise Control Engineering Journal. 2012;60(3):224-35. Epub June 2012.
10. COSMO. Consortium for Small-scale Modeling 2014. Available from: http://cosmo-model.org/.
11. International Organization of Standardization. ISO 9613-1: Acoustics - Attenuation of sound during propagation outdoors, Part 1: Calculation of the absorption of sound by the atmosphere. 1993.
12. Wunderli JM. Dokumentation des sonX Ausbreitungsmodells: Empa; 2014 [updated 15.07.2014]. Available from: http://www.empa.ch/plugin/template/empa/*/120244.
13. Polster G. Erfahrungen mit Strahlungs-, Temperaturgradient- und Windmessungen als Bestimmungsgroessen der Diffusionskategorien. Meteorologische Rundschau. 1969;6.
14. VDI. VDI 3789 Part 2: Environmental Meteorology. Interactions between Atmosphere and Surfaces, Calculation of Short-wave and Long-wave Radiation. Düsseldorf: VDI; 1994. p. 52.
15. Zellmann C, Wunderli JM, Schäffer B, editors. SonAIR - Data acquisition for a next generation aircraft noise simulation model. 42nd International Congress and Exposition on Noise Control Engineering 2013, INTER-NOISE 2013: Noise Control for Quality of Life; 2013.
16. Wunderli JM, Rotach MW. Application of statistical weather data from the numerical weather prediction model COSMO-2 for noise mapping purposes. Acta Acustica united with Acustica. 2011;97(3):403-15.
17. MeteoSwiss. Cosmo Model Properties: Dynamics and Numerics, Physics, Data Assimilation, and more ... 2014. Available from: http://www.meteoswiss.admin.ch/web/en/research/consortia/cosmo/more_about/properties.html.